AGU PUBLICATIONS

Geophysical Research Letters

RESEARCH LETTER

10.1002/2013GL058909

Key Points:
- The bulk of alluvial deposits in Gale were likely emplaced during the Hesperian
- Habitable conditions persisted in Gale crater after the Noachian
- Limited evidence for possible younger fluvial activation on Peace Vallis fan

Supporting Information:
- Readme
- Figure S1
- Figure S2
- Auxiliary Material

Correspondence to:
J. A. Grant,
grantj@si.edu

Citation:
Grant, J. A., S. A. Wilson, N. Mangold, F. Calef III, and J. P. Grotzinger (2014), The timing of alluvial activity in Gale crater, Mars, *Geophys. Res. Lett.*, *41*, 1142–1148, doi:10.1002/2013GL058909.

Received 4 DEC 2013
Accepted 22 JAN 2014
Accepted article online 28 JAN 2014
Published online 18 FEB 2014

The timing of alluvial activity in Gale crater, Mars

John A. Grant[1], Sharon A. Wilson[1], Nicolas Mangold[2], Fred Calef III[3], and John P. Grotzinger[4]

[1]Center for Earth and Planetary Studies, National Air and Space Museum, Smithsonian Institution, Washington, DC, USA, [2]Laboratoire Planetologie et Geodynamique de Nantes, LPGN/CNRS UMR6112, Universite de Nantes, Nantes, France, [3]NASA Jet Propulsion Laboratory, California Institute of Technology, Pasadena, California, USA, [4]Division of Geologic and Planetary Sciences, California Institute of Technology, Pasadena, California, USA

Abstract The *Curiosity* rover's discovery of rocks preserving evidence of past habitable conditions in Gale crater highlights the importance of constraining the timing of responsible depositional settings to understand the astrobiological implications for Mars. Crater statistics and mapping reveal the bulk of the alluvial deposits in Gale, including those interrogated by *Curiosity*, were likely emplaced during the Hesperian, thereby implying that habitable conditions persisted after the Noachian. Crater counting data sets and upper Peace Vallis fan morphology also suggest a possible younger period of fluvial activation that deposited ~10–20 m of sediments on the upper fan after emplacement of the main body of the fan. If validated, water associated with later alluvial activity may have contributed to secondary diagenetic features in Yellowknife Bay.

1. Introduction

Gale, a 154 km diameter (*D*) crater located near the Martian dichotomy boundary at 5°S, 138°E, formed in the Early Hesperian [*Irwin*, 2013] or near the time of the Noachian-to-Hesperian transition ~3.6 to 3.8 Ga [*Thomson et al*., 2011; *Le Deit et al*., 2012]. The region surrounding Gale is incised by valley networks formed in the Late Noachian to Early Hesperian [*Fassett and Head*, 2008], but these are buried by Gale's ejecta and predate the crater [*Le Deit et al*., 2012]. Gale's interior is dominated by a ~5 km high sedimentary mound (Mt. Sharp/Aeolis Mons), whose present appearance evolved in the Late Hesperian to Early Amazonian [*Kite et al*., 2013; *Wray*, 2013], but deposition of the mound materials may have occurred earlier [*Malin and Edgett*, 2000] (Figure 1). The rim of Gale is incised by valleys, and the northern wall is flanked by crater fill forming Aeolis Palus, which was emplaced by multiple processes that include alluvial [e.g., *Williams et al*., 2013], eolian, and impact contributions.

The Peace Vallis alluvial fan within the crater fill originates on the northern wall of Gale and exhibits distinct variations in morphology and thermal inertia [*Anderson and Bell*, 2010]. The upper fan unit (alluvial fan, "AF"), lower fan unit (bedded, fractured, "BF"), and distal surfaces with high crater densities (unit "CS") are mapped after *Grotzinger et al*. [2014] (Figure 1). Topographic and mapping analyses suggest that unit BF contributes to the overall form of the Peace Vallis fan deposit [*Palucis et al*., 2013] and extends into the region explored by the Mars Science Laboratory *Curiosity* [*Grotzinger et al*., 2014] (Figure 1). Thin sediments (~10–20 m) capping unit AF are bounded locally by outward facing slopes, and there is a distinct morphologic boundary between units AF and BF [*Anderson and Bell*, 2010] (Figure 1). Sinuous ridges ~0.5 to 2.5 m high [*Grotzinger et al*., 2014] on unit AF are interpreted as distributary channels now standing in relief as a result of differential erosion relative to surrounding surfaces [*Anderson and Bell*, 2010]. By contrast, unit BF lacks relict distributaries and appears more pitted and etched, and larger craters are more degraded and often expose layered sediments (Figure 1). Fans on the southwest wall of Gale are broadly similar in scale and morphology to unit AF of the Peace Vallis fan, with smooth surfaces bounded by outward facing slopes that superpose adjacent surfaces and preserve incised and inverted relict distributaries (Figure 1).

Mudstone outcrops examined by the *Curiosity* rover, informally named the Sheepbed member of the Yellowknife Bay formation, are located in a shallow (meters) topographic depression named Yellowknife Bay in the BF unit [*Grotzinger et al*., 2014]. These mudstones are consistent with deposition in a lacustrine setting and contain key textural, geochemical, and mineralogic elements that collectively provide evidence of an ancient, potentially habitable environment [*Grotzinger et al*., 2014]. The age of the Sheepbed mudstone, however, is poorly constrained relative to deposition on the Peace Vallis fan. Because the relationship between the alluvial fans, associated deposits, and other contributions to crater fill provides critical insight into the potential habitability

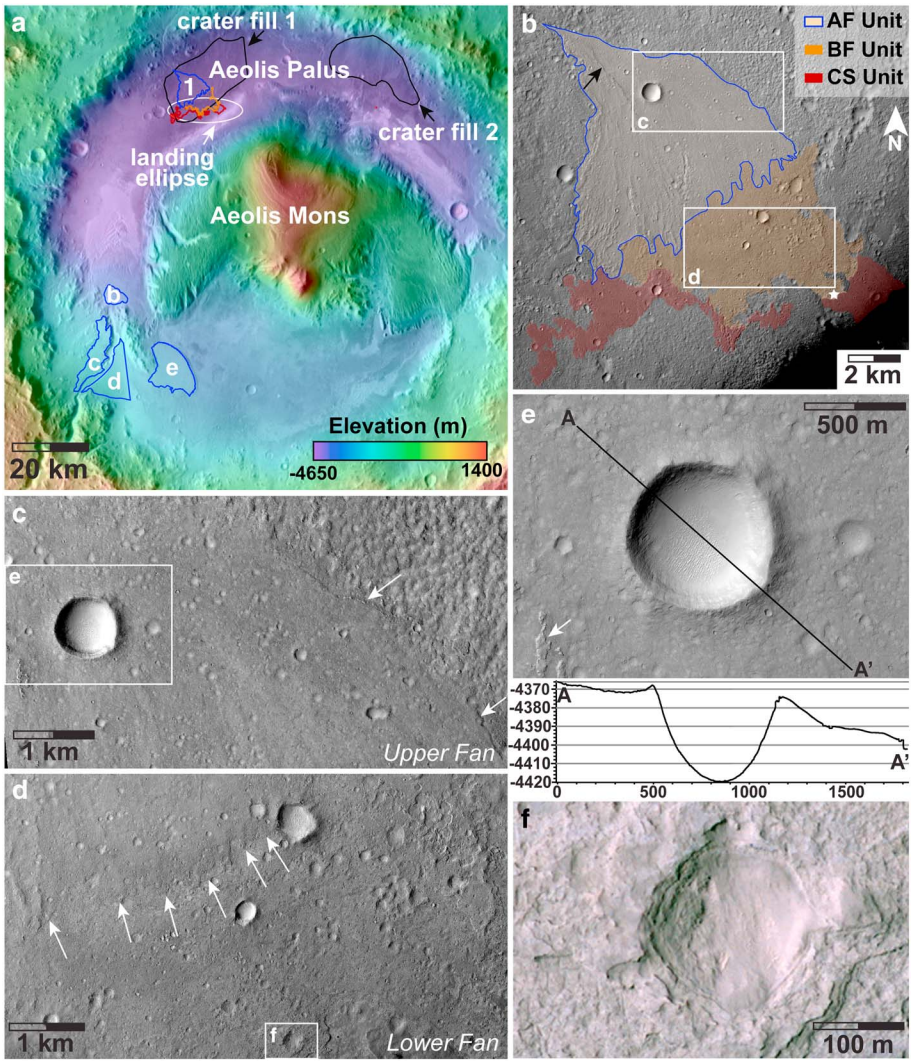

Figure 1. (a) The ~5 km high Mt. Sharp/Aeolis Mons is separated from the northern wall of Gale crater by Aeolis Palus. Crater analyses included areas on Aeolis Palus referred to as crater fill 1 (CF1) and 2 (CF2) (black outlines); fans (blue outlines) including unit AF (1), SW floor fan (2), SW upper fan north of channel (3), SW upper fan south of channel (4), SW floor fan lobe (5); and units BF (orange) and CS (red). CF1 encompasses unit AF and most of units BF and CS (Figure S1). Mars Science Laboratory landing ellipse is indicated. Mars Orbital Laser Altimeter topography over Thermal Emission Imaging System daytime IR mosaic. (b) Units AF, BF, and CS. Ridges on unit AF (e.g., black arrow) are inverted distributaries. White star shows location of Yellowknife Bay. CTX image G02_018854_1754. (c) Surface of unit AF is smooth with distinct margins (white arrows). HiRISE ESP_028269_1755. (d) Morphologic contact between units AF and BF (white arrows) [after *Anderson and Bell*, 2010] differs from contact mapped in Figure 1(b) [*Grotzinger et al.*, 2014]. Unit BF is more pitted and etched and lacks inverted channels. HiRISE ESP_028269_1755. (e) The $D \sim 750$ m crater on unit AF displays lower and thinner rim on the NW up-fan side (A) relative to the down-fan SE side (A') and appears partially buried (see profile; both scales in meters). Inverted distributary (white arrow) less than one crater diameter from rim is unaffected by the crater, suggesting that the crater is partially buried by unit AF. HiRISE ESP_026146_1755. (f) Craters on unit BF are more degraded than craters in unit AF, often exposing light-toned, layered deposits. HiRISE PSP_010573_1755 (color). North toward top in all images.

when they formed [e.g., *Williams et al.*, 2013], this study establishes the timing of alluvial activity in Gale as it may relate to rocks explored in Yellowknife Bay [*Grotzinger et al.*, 2014].

2. Methods

We combine geologic mapping and crater statistics to interpret ages of "crater fill" (CF1 and CF2) comprising Aeolis Palus; units AF, BF, and CS; and other alluvial fans in Gale to place them in a broader geologic framework. Areas used are based on prior mapping [*Anderson and Bell*, 2010; *Grotzinger et al.*, 2014], assessment of

morphologic and (or) topographic data, and the juxtaposition of landforms (supporting information). Crater statistics were compiled in ArcGIS using data from the Context Camera (CTX) [*Malin et al*., 2007] on the Mars Reconnaissance Orbiter and CraterTools software [*Kneissl et al*., 2011]. The 6 m/pixel scale of CTX data enabled confident definition of craters >20 m in diameter, and counts excluded obvious secondary clusters (supporting information). Counts were completed on individual CTX images to minimize variable lighting and image quality effects. To further reduce effects of image resolution, craters with D <50 m were counted but excluded from interpretation of ages. Interpreted ages for each count were derived from segments of the plots for each unit that best match the expected production population using "pseudo-log" binned reverse cumulative histograms and Craterstats2 software [*Michael and Neukum*, 2010]. Absolute ages are based on the chronology function of *Hartmann and Neukum* [2001] and production function from *Ivanov* [2001]. Uncertainty in the timing of the Hesperian-to-Amazonian transition was also incorporated (supporting information). Ages were also interpreted from the incremental plots using the variable diameter bin-size method of *Hartmann* [2005] (Table S1). Areas used are very small, thereby introducing uncertainty in the absolute interpretation of individual counts. However, combining and comparing areas for units inferred to be of similar age and origin (e.g., alluvial fans) enables robust interpretations.

3. Results

Cumulative statistics for CF1 and CF2 (307 and 236 km^2, respectively) on Aeolis Palus approach the expected production population [*Ivanov*, 2001] at diameters over 200 m but are relatively deficient in smaller craters (Figure 2a, left, and supporting information). Craters >200 m in diameter are uniformly distributed across the crater fill areas (Figure S1). We believe craters >400 m in diameter for both crater fill areas (12 craters and 7 craters for CF1 and CF2, respectively; Table S1) give the best fit to the expected production population and yield interpreted ages in the middle of the Hesperian. Modeled absolute ages are in the range of ~3.3 to 3.2 Ga, consistent with the inferred Early Hesperian age for the cratered unit on the floor of Gale [e.g., *Thomson et al*., 2011]. Inclusion of craters >300 m across yields slightly younger ages (Table S1). Incremental statistics are similar, showing a deficiency of craters with diameters smaller than ~300 m relative to the expected production population (Figure 2a, right).

Crater statistics for units AF (~49 km^2), BF (31 km^2), and CS (15.5 km^2) [*Grotzinger et al*., 2014] were compiled using very small areas, so caution is required when making interpretations (Figure 2b). To provide further insight, the ages of three morphologically distinct fans (areas 22 to 111 km^2) on Gale's floor were analyzed (Figures 1 and 2c and supporting information). Most of these alluvial surfaces are dominated by craters <200 m across, with the notable exception of a ~750 m diameter crater on unit AF, and the number of craters larger than 30 m in diameter included in each count increases with area (Figures 2 and S2).

The cumulative plots for craters on unit AF achieve a production population of craters with diameters between 90 to 150 m and yield an age corresponding to the Amazonian (Figures 2b and S2). By contrast, plots for the distinct BF and CS units do not provide a good match to the expected production population at any significant diameter range and show a more continuous decrease in craters at decreasing diameters relative to the production population (Figures 2b and S2 and Table S1). For example, fits to crater diameters between 90 and 170 m are poor for unit BF and yield Amazonian ages, whereas use of larger crater diameters are also a poor fit and yield ages approaching the Hesperian (Table S1), thereby suggesting they could be older than unit AF. Plots for fans in southwest Gale yield Amazonian ages broadly comparable to unit AF (Table S1), and combining them using craters >120 m in diameter gives a better fit to the production population that correlates to an age of ~1.2 Ga (Figure 2c, left). Inclusion of smaller craters yields slightly younger ages (Table S1). Incremental statistics for unit AF and the southwest fans are less definitive about later activity and are generally similar to the crater fill areas at crater diameters >200 m: the crater fill shows a deficiency of craters with D < 200 m relative to the fans and the expected production population.

The incremental plots for most counts yield comparable to slightly younger ages than the cumulative plots (Figure 2 and Table S1) due to differences in the production function and position of hypothesized isochrones [*Hartmann*, 2005; *Carr*, 2006] and small differences in the diameter ranges used for some counts that we interpreted to best fit the crater data. With the understanding that interpreted ages represent the minimum age of the surface (end of geomorphic activity), we emphasize the older values derived from the cumulative statistics (Figures 2 and S2 and Table S1).

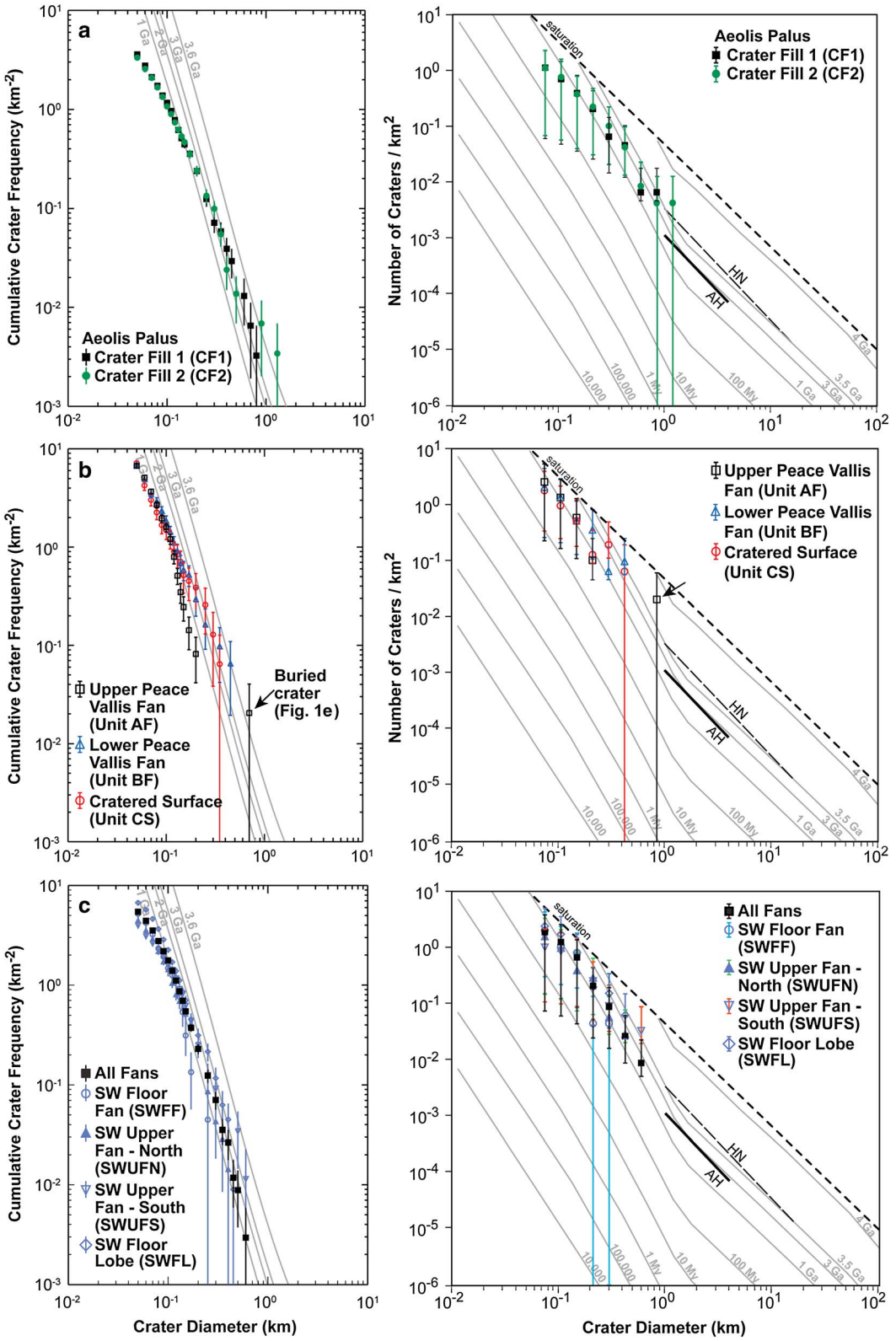

Figure 2. (left) Cumulative and (right) incremental crater size frequency distributions for (a) crater fill areas on Aeolis Palus; (b) Units AF (black arrow denotes $D \sim 750$ m crater discussed in text but not included in interpretation of unit AF age), BF, and CS; and (c) fans in southwest Gale (Figure 1 and supporting information). "All Fans" includes data from fans "1" through "5" (Figure 1). Amazonian-Hesperian (AH) and Hesperian-Noachian (HN) boundaries are indicated. Error bars reflect $\pm 1/N^{0.5}$ and $N \pm N^{0.5}/A$ for data in cumulative and incremental plots, respectively (N = number of craters; A = area).

4. Discussion

Overall, cumulative statistics for the Aeolis Palus crater fill reveal crater numbers approaching the expected production population for crater diameters over ~200 m (Figure 2). By contrast, crater numbers on fan surfaces vary as a function of area. For example, individual counts approach the production population at diameters of 150 m to 90 m for unit AF versus 300 m to 120 m on the broader SW upper fan south (Figure 1 and Table S1). The production population in the crater fill is best observed in craters $D > 400$ due to more, larger craters resulting from larger counting areas. Interpretation of statistics from unit AF is complicated by the presence of a $D \sim 750$ m crater (Figure 1), but the up-fan rim on the NW side is only 4 m high and ~100 m wide, less than the expected range of ~20 m high and ~300 m wide for a crater that size [*Melosh*, 1989]. By contrast, rim height and width are closer to expected values on the down-fan SE side (lesser asymmetry persists after detrending local slope). Coupled with the pristine rim crest, absence of ejecta, and lack of influence on a relict distributary less than one crater diameter to the SW, this argues the crater predates the exposed fan surface and is therefore excluded from the unit AF statistics.

Statistics for the larger diameter craters on the Aeolis Palus crater fill indicate that infilling began shortly after the crater formed and ended in the Hesperian, likely ~3.3 to 3.2 Ga. Active processes included transport and deposition of alluvial sediments, as demonstrated by upslope valleys around the crater rim [*Anderson and Bell*, 2010], and perhaps deposition of the materials forming Aeolis Mons if it was once more extensive [*Malin and Edgett*, 2000] rather than having evolved in place [*Kite et al*., 2013]. Burial by such a deposit is consistent with the cemented nature of many of the rocks investigated by *Curiosity* [*Grotzinger et al*., 2014; *Williams et al*., 2013]. Preservation of the Early-to-middle of the Hesperian-aged crater fill surface, however, precludes a significant period of later degradation.

Preservation of the Hesperian age surface across Aeolis Palus is demonstrated by the larger-diameter craters in the crater fill counts. The uniform distribution of craters $D > 200$ m across the surface (Figure S1) constrains post-Hesperian erosion and (or) deposition to ~20–40 m based on a depth-to-diameter ratio of 0.2 for primary and 0.1 for secondary craters, respectively [*Melosh*, 1989]. Although local erosion may exceed this amount, more significant widespread erosion or deposition would lead to gaps in the distribution of larger craters.

If Aeolis Mons were once part of a thick, more extensive deposit [*Malin and Edgett*, 2000], the preserved distribution of larger craters on the crater fill requires that associated deposition and partial erosion (to its present extent) occurred during the Hesperian. More significant local erosion or deposition (including local deposits associated with Aeolis Mons) cannot be ruled out, but these results require that the current surface of Aeolis Palus and the expression of the Peace Vallis fan were largely established in the Hesperian.

Cumulative crater statistics for craters with $D > 120$ m on unit AF and fans to the southwest are consistent with a possible later period of degradation approximately correlating with establishment of the current form of Aeolis Mons [*Kite et al*., 2013; *Wray*, 2013] in the Amazonian. The occurrence of relict distributaries on unit AF suggests that late alluvial activity was possible. Moreover, relief on these distributaries plus an additional ~2–3 m to account for original channel depth confirms <5 m deflation. Finally, the absence of pedestal craters or depositional remnants indicates that such activity on unit AF was not dominated by eolian processes (e.g., final shaping of Aeolis Mons).

The distinct morphological boundaries between unit AF relative to adjacent surfaces and unit BF is consistent with a younger, less eroded surface that may have formed during a period of late aqueous activity. Preservation of the uniform distribution of larger craters on Aeolis Palus (CF1 and CF2) requires that any later alluvial deposition resulted in only 20–40 m of sediments. This is consistent with the thin (meters thick) nature of unit AF inferred from its smooth expression, low outward facing margins (Figure 1), and the inferred ~15 m burial of the upslope rim of the ~750 m diameter crater on unit AF. About 5 m of erosion is required to account for topographic inversion of putative distributary channels in unit AF and is consistent with erosion predicted by the relative deficiency of craters <30 m across on unit AF (for depth-to-diameter ratios of 0.1 to 0.2 [*Melosh*, 1989]).

By contrast, *Curiosity* measured 18 m of relief over a 450 m traverse in unit BF [*Grotzinger et al*., 2014], which is consistent with expected erosion of the crater fill since the Early to middle of the Hesperian. This implies that unit BF may be older and (or) composed of significantly less resistant materials than unit AF. Moreover, the relatively low slope of the crater size-frequency distribution from unit BF suggests more continuous erosion since the end of early aqueous activity, which is consistent with its more eroded morphology relative to unit AF.

Although unit BF may be less resistant than unit AF, unit CS appears more resistant based on preservation of meter-scale blocks around larger craters and retention of smaller craters whose numbers match the expected production population. Nevertheless, outcrops in unit CS do not significantly alter the surface topographic profile, thereby implying observed relief accommodates the relative resistance of these materials. Any late aqueous activity remains speculative due to small areas considered, similar number of craters with $D > 200$ m in the incremental statistics for unit AF and other fans and crater fill, and the possibility that differences in the expression of unit BF relate to depositional and (or) material properties.

5. Implications for Habitability

Deposition of the crater fill forming Aeolis Palus likely occurred in the Hesperian, as suggested by crater statistics and preservation of a uniform distribution of craters >200 m across. Moreover, rocks comprising unit BF were likely deposited during this time based on their eroded appearance and relief measured over *Curiosity*'s traverse that matches expected erosion. Although uncertain, crater statistics for unit BF are consistent with their being older. If the rocks in Yellowknife Bay (unit BF) were emplaced in the middle of the Hesperian (~3.3 to 3.2 Ga), then the habitable environments they record occurred relatively late in Martian history and may not have been isolated [e.g., *Mangold et al*., 2012], indicating such conditions persisted at least locally after the Noachian [*Grotzinger et al*., 2014].

The crater counting data sets and morphology of unit AF suggest a possible younger period of Peace Vallis fan activation after the emplacement of the main body of the fan, resulting in ~10–20 m deposition on unit AF. Any late activity was perhaps concurrent with establishment of the present-day form of Aeolis Mons [*Wray*, 2013] and late alluvial contributions to fans elsewhere [*Grant and Wilson*, 2011, 2012; *Morgan et al*., 2013]. Based on morphology, it is unlikely that any late alluvial deposition extended to unit BF or Yellowknife Bay, though associated water could have contributed to secondary diagenetic features observed by *Curiosity* [*Grotzinger et al*., 2014]. Evaluation of any potentially associated habitable settings requires more confident interpretation of the occurrence, timing, and extent of late activity and sampling of resultant deposits.

Acknowledgments
We thank the Jet Propulsion Laboratory, University of Arizona, Ball Aerospace, Malin Space Science Systems, and Lockheed Martin that built and operate the *Curiosity* rover, HiRISE and CTX cameras, and the Mars Reconnaissance Orbiter. Reviews by Devon Burr and David Crown improved this paper. This work was supported by NASA.

The Editor thanks Devon Burr and David Crown for their assistance in evaluating this paper.

References

Anderson, R. B., and J. F. Bell III (2010), Geologic mapping and characterization of Gale crater and implications for its potential as a Mars Science Laboratory landing site, *Mars*, *5*, 76–128, doi:10.1555/mars.2010.0004.

Carr, M. H. (2006), *The Surface of Mars*, 307 pp., Cambridge Univ. Press, Cambridge, U. K.

Fassett, C. I., and J. W. Head (2008), The timing of Martian valley network activity: Constraints from buffered crater counting, *Icarus*, *195*, 61–89, doi:10.1016/j.icarus.2007.12.009.

Grant, J. A., and S. A. Wilson (2011), Late alluvial fan formation in southern Margaritifer Terra, Mars, *Geophys. Res. Lett.*, *38*, L08201, doi:10.1029/2011GL046844.

Grant, J. A., and S. A. Wilson (2012), A possible synoptic source of water for alluvial fan formation in southern Margaritifer Terra, Mars, *Planet. Space Sci.*, *72*, 44–52, doi:10.1016/j.pss.2012.05.020.

Grotzinger, J. P., et al. (2014), A habitable fluvio-lacustrine environment at Yellowknife Bay, Gale Crater, Mars, *Science*, *343*(6169), 1–14, doi:10.1126/science.1242777.

Hartmann, W. K. (2005), Martian cratering 8: Isochron refinement and the chronology of Mars, *Icarus*, *174*, 294–320.

Hartmann, W. K., and G. Neukum (2001), Cratering chronology and the evolution of Mars, *Space Sci. Rev.*, *96*, 165–194.

Irwin, R. P. (2013), Testing links between impacts and fluvial erosion on post-Noachian Mars, *LPS XLIV*, 2958.

Ivanov, B. A. (2001), Mars/Moon cratering ratio estimates, *Space Sci. Rev.*, *96*, 87–104.

Kite, E. S., K. W. Lewis, M. P. Lamb, C. E. Newman, and M. I. Richardson (2013), Growth and form of the mound in Gale Crater, Mars: Slope wind enhanced erosion and transport, *Geology*, *41*, 543–546, doi:10.1130/G33909.1

Kneissl, T., S. van Gasselt, and G. Neukum (2011), Map-projection-independent crater size-frequency determination in GIS environments—New software tool for ArcGIS, *Planet. Space Sci.*, *59*, 1243–1254, doi:10.1016/j.pss.2010.03.015.

Le Deit, L., E. Hauber, F. Fueten, N. Mangold, M. Pondrelli, A. Rossi, and R. Jaumann (2012), Model age of Gale crater and origin of its layered deposits, *3rd Int. Early Mars*, 7045.

Malin, M. C., and K. S. Edgett (2000), Sedimentary rocks of early Mars, *Science*, *290*, 1927–1937, doi:10.1126/science.290.5498.

Malin, M. C., et al. (2007), Context Camera investigation on board the Mars Reconnaissance Orbiter, *J. Geophys. Res.*, *112*, E06S04, doi:10.1029/2006JE002808.

Mangold, N., S. Adeli, S. Conway, V. Ansan, and B. Langlais (2012), A chronology of early Mars climatic evolution from impact crater degradation, *J. Geophys. Res.*, *117*, E04003, doi:10.1029/2011JE004005.

Melosh, H. J. (1989), *Impact Cratering*, 245 pp., Oxford Univ. Press, New York.

Michael, G. G., and G. Neukum (2010), Planetary surface dating from crater size-frequency distribution measurements: Partial resurfacing events and statistical age uncertainty, *Earth Planet. Sci. Lett.*, *226*, 885–890, doi:10.1016/j.epsl.2009.12.041.

Morgan, A. M., A. D. Howard, D. E. J. Hobley, J. M. Moore, W. E. Dietrich, R. M. E. Williams, D. M. Burr, J. A. Grant, S. A. Wilson, and Y. Matsubara (2013), Sedimentology and climatic environment of alluvial fans in the Martian Saheki crater and a comparison with terrestrial fans in the Atacama Desert, *Icarus*, *229*, 131–156.

Palucis, M. C., W. E. Dietrich, A. Hayes, R. M. E. Williams, F. Calef, D. Y. Sumner, S. Gupta, C. Hardgrove, and MSL Science Team (2013), Origin and evolution of the Peace Vallis fan system that drains into the Curiosity landing area, Gale crater, *LPS XLIV*, 1607.

Thomson, B. J., N. T. Bridges, R. Milliken, A. Baldridge, S. J. Hook, J. K. Crowley, G. M. Marion, C. R. de Souza Filho, A. J. Brown, and C. M. Weitz (2011), Constraints on the origin and evolution of the layered mound in Gale Crater, Mars using Mars Reconnaissance Orbiter data, *Icarus*, *214*, 413–432, doi:10.1016/j.icarus.2011.05.002.

Williams, R. M. E., et al. (2013), Martian fluvial conglomerates at Gale crater, *Science*, *340*, 1068–1072, doi:10.1126/science.1237317.

Wray, J. J. (2013), Gale crater: The Mars Science Laboratory/Curiosity Rover landing site, *Int. J. Astrobiol.*, *12*, 25–38, doi:10.1017/S1473550412000328.